TOPOLOGICAL ASYMPTOTIC ANALYSIS OF A DIFFUSIVE-CONVECTIVE-REACTIVE PROBLEM

D. RUSCHEINSKY, F. S. CARVALHO, C. T. M. ANFLOR, AND A.A. NOVOTNY

Abstract.
Purpose Sensitivity analysis of the L^2-norm and H^1-seminorm of the solution of a diffusive-convective-reactive problem to topological changes of the underlying material.
Design/methodology/approach The topological derivative method is used to devise a simple and efficient topology design algorithm based on a level-set domain representation method.
Findings Remarkably simple analytical expressions for the sensitivities are derived, which are useful for practical applications including heat exchange topology design and membrane eigenvalue maximization.
Originality/value The topological asymptotic expansion associated with a diffusive-convective-reactive equation is rigorously derived, which is not available in the literature yet.

1. Introduction

The topological derivative (TD) is defined as the first term (correction) of the asymptotic expansion of a given shape functional with respect to a small parameter that measures the size of singular domain perturbations, such as holes, inclusions, source-terms and cracks (Novotny and Sokołowski, 2013). This relatively new concept has applications in many different fields such as shape and topology optimization (Lopes et al., 2017; Anflor et al., 2018), inverse problems (Ferreira and Novotny, 2017), imaging processing (Hintermüller and Laurain, 2009), multi-scale material design (Amstutz et al., 2010) and mechanical modeling including damage and fracture evolution phenomena (Ammari et al., 2013; Xavier et al., 2017). Topological derivative was conceived as a family of methods governed by a threshold approach. More recently, it has been successfully combined with a level-set domain representation method (Amstutz and Andrä, 2006), leading to a very simple and quite efficient one-stage topology design algorithm driven by the topological derivative only. For an account on the theoretical development and applications of the topological derivative method, see the series of review papers (Novotny et al., 2019a,b,c). See also (Bojczuk and Mróz, 2012; Giusti et al., 2017; Norato et al., 2007; Otomori et al., 2015). Despite not been cited there are many other works with relevant contribution in the advances in the topological derivative field.

However, the topological asymptotic expansion for the modified diffusive-convective-reactive equation is not available in the literature. This equation allows for solving problems such as design of heat exchangers and structural eigenvalue optimization. In fact, some structures in the nature present branching tree or dendritic shapes. This class of problems has been first introduced as constructal law with the proposal to recognize that there is a universal phenomenon that generates an optimum configuration of design in nature (Bejan et al., 1995; Bejan, 1997). This phenomenon can be observed by topology optimization when solving the steady-state heat conduction problems, where the majority of studies also confirm that the dendritic structures represent a class of optimal design (Bendsøe and Sigmund, 2003; Gersborg-Hansen et al., 2006; Lohan et al., 2017). Dbouk (2017) presents a survey review about the topology methods developed during the last 15 years for optimizing problems considering conductive, convective and conjugate heat

Key words and phrases. topological derivative, diffusive/convective/reactive problem, heat exchange topology design, membrane eigenvalue maximization, asymptotic analysis.

transfer. This paper discusses some aspects regarding the numerical methodologies developed to result in an optimum design with complex geometries and their natural industrial manufacturing drawback. The optimum design of heat exchangers are still being considered in the literature as well as the development of numerical approaches to obtain the optimized final geometry with fine-tune designs. On the other hand, the eigenvalue problem in structural optimization plays an important role in structural integrity. When the frequency of excitation is tuned to one of the natural frequencies of vibration the structure can be damaged or even collapse. In this sense, problems of optimization are formulated as the maximization of the smallest eigenvalue subjected to a global constraint. According to the literature, structures can present simple or multiple eigenvalues. Methods to deal with simple eigenvalue are well established and are quite simple to be implemented in a topology optimization routine. The main problem in a topology optimization is that at the initial iterations only simple eigenvalues are present but as the iterative process evolves the geometry becomes complex and multiple eigenvalues may arise. Masur and Mróz (1979) and Haug and Rousselet (1980) demonstrated that multiple eigenvalues are not differentiable in the common sense, creating serious problems for derivation of optimality conditions and numerical analysis in solving optimization problems. Complex geometries require specific methods to deal with optimum structural design with respect to multiple eigenvalues due to the several numbers of design parameters and many degrees of freedom. Seyranian et al. (1994) presented a numerical methodology for calculating the design sensitivity by changing all design parameters simultaneously. Since then, several numerical and analytical works have been suggested to solve problems involving simple and multiple eigenvalues by, among others Ammari and Khelifi (2003); Huang et al. (2010); Li et al. (2016). In particular, the topological derivative for simple eigenvalues of the Laplacian was considered by Ammari and Khelifi (2003) and for multiple eigenvalues in the context of elasticity system by Nazarov and Sokolowski (2008).

Therefore, in the work, the topological asymptotic analysis of the L^2-norm and H^1-seminorm of the solution to a diffusive-convective-reactive problem, with respect to nucleation of inclusions endowed with different material properties from the background, is considered. The associated bilinear form becomes non-symmetric and non-coercive. How to deal with these issues represents the main challenge of this work. In addition, the resulting topological derivatives are used to devise a topology design algorithm based on a level-set domain representation method. Finally, two numerical examples are presented. The first one consists in a heat exchange topology design and the second example shows an application in the context of membrane eigenvalue maximization. In particular, the paper is organized as follows. Section 2 presents a brief review on the topological derivative method. The mathematical formulation for the proposed problem as well as the proof of existence of the associated topological derivative are introduced in Section 3. The main results of the paper are stated through Theorems 1 and 2 in Section 4. The obtained sensitivities are adapted to some selected applications in Section 5. Numerical examples are presented to demonstrate the effectiveness of the obtained topological derivatives in Section 6. Finally, Section 7 draws some concluding remarks. Rigorous mathematical justification for the derived results are presented in Appendix A, including appropriated estimates for the remainders left in the topological asymptotic expansions.

2. The Topological Derivative Concept

Let us consider an open and bounded domain $\Omega \subset \mathbb{R}^2$ which is subject to a nonsmooth perturbation confined in a small ball $B_\varepsilon(\widehat{x})$ of radius ε and center at $\widehat{x} \in \Omega$. We introduce a characteristic function $x \mapsto \chi(x)$ associated to the unperturbed domain, namely $\chi = \mathbb{1}_\Omega$ such that

$$|\Omega| = \int_\Omega \chi, \tag{2.1}$$

where $|\Omega|$ is the Lebesgue measure of Ω. Then, we define a characteristic function associated to the topologically perturbed domain of the form $x \mapsto \chi_\varepsilon(\widehat{x}, x)$. In the case of a perforation, for instance $\chi_\varepsilon(\widehat{x}) = \mathbb{1}_\Omega - \mathbb{1}_{B_\varepsilon(\widehat{x})}$ and the singulary perturbed domain is given by $\Omega_\varepsilon = \Omega \backslash \overline{B_\varepsilon}$. Then, we assume that a given shape functional $\psi(\chi_\varepsilon(\widehat{x}))$, associated to the topologically perturbed domain, admits the following topological asymptotic expansion

$$\psi(\chi_\varepsilon(\widehat{x})) = \psi(\chi) + f(\varepsilon) D_T \psi(\widehat{x}) + o(f(\varepsilon)), \tag{2.2}$$

where $\psi(\chi)$ is the shape functional associated to the unperturbed domain, $f(\varepsilon)$ is a positive first order correction function of ψ and $o(f(\varepsilon))$ is the remainder, namely $o(f(\varepsilon))/f(\varepsilon) \to 0$ with $\varepsilon \to 0$. The function $\widehat{x} \mapsto D_T \psi(\widehat{x})$ is called the topological derivative of ψ at $\widehat{x}$. Therefore, this derivative can be seen as a first order correction of $\psi(\chi)$ to approximate $\psi(\chi_\varepsilon(\widehat{x}))$.

3. Problem Formulation

In this section, the mathematical model for the diffusive-convective-reactive problem, as well as the shape functionals we are dealing with, are introduced. The original unperturbed and topologically perturbed problems are stated, together with arguments on the existence of the associated topological derivative.

3.1. **Unperturbed problem.**

The original unperturbed problem is stated as:

$$u \in H^1_0(\Omega) : \int_\Omega \alpha \nabla u \cdot \nabla \eta + \int_\Omega \beta (\nabla u \cdot V) \eta + \int_\Omega \rho k u \eta = \int_\Omega f \eta \quad \forall \eta \in H^1_0(\Omega), \tag{3.1}$$

where α, β, ρ and k are positive and bounded functions, f is a distributed source and V is a given vector field, such that, $\operatorname{div}(V) = 0$ in Ω and $V \cdot n = 0$ on $\partial\Omega$. The quantities α, β, ρ, k and f are assumed to be piecewise constant functions as described in Table 1, where $\omega \subset \Omega$. Precise physical meaning of (3.1) is given in Sections 5.1 and 5.2. The auxiliaries

Table 1. Values of α, β, ρ and f.

	α	β	ρ	f
$\Omega \setminus \omega$	α_0	β_0	ρ_0	f_0
ω	α_1	β_1	ρ_1	f_1

shape functionals are defined by,

$$\mathcal{G}(u) = \int_\Omega \rho k u^2 \qquad \text{and} \qquad \mathcal{J}(u) = \int_\Omega \alpha \|\nabla u\|^2. \tag{3.2}$$

In order to simplify further analysis, we introduce the adjoint problems

$$q \in H^1_0(\Omega) : \int_\Omega \alpha \nabla q \cdot \nabla \eta - \int_\Omega \beta (\nabla q \cdot V) \eta + \int_\Omega \rho k q \eta = -2 \int_\Omega \rho k u \eta, \quad \forall \eta \in H^1_0(\Omega), \tag{3.3}$$

$$p \in H^1_0(\Omega) : \int_\Omega \alpha \nabla p \cdot \nabla \eta - \int_\Omega \beta (\nabla p \cdot V) \eta + \int_\Omega \rho k p \eta = -2 \int_\Omega \alpha \nabla u \cdot \nabla \eta, \quad \forall \eta \in H^1_0(\Omega). \tag{3.4}$$

3.2. **Perturbed problem.** The topological perturbation is defined according to Tables 2 and 3, where $B_\varepsilon(\widehat{x}) = \{\|x - \widehat{x}\| < \varepsilon\}$ for $\widehat{x} \in \Omega$ and $\omega \subset \Omega$. From these elements, the topologically perturbed problem is stated as,

$$u_\varepsilon \in H^1_0(\Omega) : \int_\Omega \alpha_\varepsilon \nabla u_\varepsilon \cdot \nabla \eta + \int_\Omega \beta_\varepsilon (\nabla u_\varepsilon \cdot V)\eta + \int_\Omega \rho_\varepsilon k u_\varepsilon \eta = \int_\Omega f_\varepsilon \eta \quad \forall \eta \in H^1_0(\Omega), \quad (3.5)$$

with $V \cdot n = 0$ on ∂B_ε. The auxiliary shape functionals in perturbed domain are defined by

$$\mathcal{G}_\varepsilon(u_\varepsilon) = \int_\Omega \rho_\varepsilon k u_\varepsilon^2 \qquad \text{and} \qquad \mathcal{J}_\varepsilon(u_\varepsilon) = \int_\Omega \alpha_\varepsilon \|\nabla u_\varepsilon\|^2. \quad (3.6)$$

Remark 1. *The following result is important for the development of the work. Let* $\varphi \in H^1_0(\Omega)$ *then*

$$\int_\Omega 2(\nabla \varphi \cdot V)\varphi = \int_\Omega \operatorname{div}(V|\varphi|^2) - \int_\Omega \operatorname{div}(V)|\varphi|^2 = \int_{\partial\Omega} (V \cdot n)|\varphi|^2 = 0, \quad (3.7)$$

provided that $\operatorname{div}(V) = 0$.

TABLE 2. Values of α_ε, β_ε, ρ_ε and f_ε.

	α_ε	β_ε	ρ_ε	f_ε
$\Omega \setminus B_\varepsilon$	α	β	ρ	f
B_ε	$\gamma_\alpha \alpha$	$\gamma_\beta \beta$	$\gamma_\rho \rho$	$\gamma_f f$

TABLE 3. Values of γ_α, γ_β, γ_ρ and γ_f.

	γ_α	γ_β	γ_ρ	γ_f
$\Omega \setminus \omega$	α_1/α_0	β_1/β_0	ρ_1/ρ_0	f_1/f_0
ω	α_0/α_1	β_0/β_1	ρ_0/ρ_1	f_0/f_1

3.3. **Existence of the topological derivative.** The shape functionals in the original and perturbed domains are introduced through equations (3.1) and (3.5), respectively. Now, it is possible to state the following result associated with the existence of the topological derivative for the problem under analysis:

Lemma 1. *Let* u *and* u_ε *be solutions to the original* (3.1) *and perturbed* (3.5) *problems, respectively.Then the estimate* $\|u_\varepsilon - u\|_{H^1(\Omega)} = O(\varepsilon)$ *holds true.*

Proof. Initially (3.1) is subtracted from the perturbed problem (3.5). After some analytical manipulations taking into account the contrast (Tables 2 and 3), and by setting $\eta = u_\varepsilon - u$, one can obtain

$$\int_\Omega \alpha_\varepsilon \|\nabla(u_\varepsilon - u)\|^2 + \int_\Omega \rho_\varepsilon k |u_\varepsilon - u|^2 = \int_{B_\varepsilon} (1 - \gamma_\alpha)\alpha \nabla u \cdot \nabla(u_\varepsilon - u) + \int_{B_\varepsilon} (1 - \gamma_\beta)\beta(\nabla u \cdot V)(u_\varepsilon - u) + \int_{B_\varepsilon} (1 - \gamma_\rho)\rho k u(u_\varepsilon - u) - \int_{B_\varepsilon} (1 - \gamma_f) f(u_\varepsilon - u). \quad (3.8)$$

since $\operatorname{div}(V) = 0$ and $V \cdot n = 0$ on ∂B_ε. Using the equality (3.8) and the Cauchy-Schwarz inequality, results in

$$\int_\Omega \alpha_\varepsilon \|\nabla(u_\varepsilon - u)\|^2 + \int_\Omega \rho_\varepsilon k |u_\varepsilon - u|^2 \leqslant C_1 \varepsilon \|u_\varepsilon - u\|_{H^1(\Omega)}. \quad (3.9)$$

From the coercivity of the bilinear form on the left-hand side of (3.9), we have

$$c\|u_\varepsilon - u\|^2_{H^1(\Omega)} \leq \int_\Omega \alpha_\varepsilon \|\nabla(u_\varepsilon - u)\|^2 + \int_\Omega \rho_\varepsilon k |u_\varepsilon - u|^2, \tag{3.10}$$

which leads to the result

$$\|u_\varepsilon - u\|_{H^1(\Omega)} \leqslant C\varepsilon, \tag{3.11}$$

with the constant $C = C_1/c$ independent of the small parameter ε. □

4. Topological Sensitivities

Before stating the two main results of the paper, let us introduce the following second-order polarization tensors

$$\mathbf{P}_\alpha = \frac{1-\gamma_\alpha}{1+\gamma_\alpha}\mathbf{I} \quad \text{and} \quad \mathbf{P}_{\alpha\beta} = \frac{1-\gamma_\beta}{1+\gamma_\alpha}\mathbf{I}, \tag{4.1}$$

associated with the contrast on the diffusive γ_α and convective γ_β terms. From the problems presented in (3.1) and (3.5) two results are formulated, related to the topological derivative. The proofs of the following theorems are presented in the Appendix A.

Theorem 1. *Let $\mathcal{G}(u)$ be the shape functional defined in* (3.2)*-left, then its associated topological derivative is given by*

$$D_T\mathcal{G} = -2\alpha\mathbf{P}_\alpha\nabla u\cdot\nabla q - 2\beta(\mathbf{P}_{\alpha\beta}\nabla u\cdot V)q - \rho k(1-\gamma_\rho)u(u+q) + (1-\gamma_f)qf, \tag{4.2}$$

where q is the adjoint state solution of (3.3)*.*

Theorem 2. *Let $\mathcal{J}(u)$ be the shape functional presented in* (3.2)*-right. Then, the topological derivative of $\mathcal{J}$ is given by*

$$D_T\mathcal{J} = -2\alpha\mathbf{P}_\alpha\nabla u\cdot\nabla(u+p) - 2\beta(\mathbf{P}_{\alpha\beta}\nabla u\cdot V)p - \rho k(1-\gamma_\rho)up + (1-\gamma_f)pf, \tag{4.3}$$

where p is the adjoint solution of problem (3.4)*.*

5. Selected Applications

The topological derivatives of the L^2-norm and H^1-seminorm of the solution to a diffusive-convective-reactive problem, with respect to nucleation of inclusions endowed with different material properties of the background, have been presented in Section 4. The topological asymptotic formalism enables straightforward extensions of these results to other elliptic operators and shape functionals. In this section, two selected examples are considered. The first one consists in a heat exchange topology design and the second example shows an application in the context of membrane eigenvalue maximization.

5.1. **Diffusion-Convection equation.** We are interested in the diffusion-convection problem which can be stated as: Find u, such that

$$\left\{\begin{array}{rcll} -\mathrm{div}(\alpha\nabla u) + \beta(\nabla u\cdot V) &=& f & \text{in } \Omega\,, \\ u &=& 0 & \text{on } \Gamma_D, \\ \partial_n u &=& 0 & \text{on } \Gamma_N. \end{array}\right. \tag{5.1}$$

Therefore, u represents the temperature field, whereas α is the diffusion coefficient, β is the convection coefficient and V is a given velocity field.

Let us consider the following shape functional

$$\mathcal{F}(u) = \tau\int_\Omega \alpha\|\nabla u\|^2 + (1-\tau)\int_\Omega \rho|u|^2, \tag{5.2}$$

with $0 \leqslant \tau \leqslant 1$ and u solution to (5.1). Then, its associated topological derivative, by taking into account contrasts on α and ρ (and not on β as well as on f), is given by

$$D_T\mathcal{F} = -2\alpha\mathbf{P}_\alpha\nabla u\cdot(\tau\nabla u + \nabla p + \nabla q) - (1-\tau)(1-\gamma_\rho)\rho|u|^2, \tag{5.3}$$

where p and q are respectively solutions of the following adjoint problems

$$p \in \mathcal{U}(\Omega) : \int_\Omega \alpha \nabla p \cdot \nabla \eta - \int_\Omega (\nabla p \cdot V)\eta = -2\tau \int_\Omega \alpha \nabla u \cdot \nabla \eta \quad \forall \eta \in \mathcal{U}(\Omega), \tag{5.4}$$

$$q \in \mathcal{U}(\Omega) : \int_\Omega \alpha \nabla q \cdot \nabla \eta - \int_\Omega (\nabla q \cdot V)\eta = -2(1-\tau) \int_\Omega \rho u \eta \quad \forall \eta \in \mathcal{U}(\Omega), \tag{5.5}$$

with the space $\mathcal{U}(\Omega) = \{\varphi \in H^1(\Omega) : \varphi_{|\Gamma_D} = 0\}$.

5.2. **Eigenvalue of the Laplace problem.** The eigenvalue of the Laplace problem modeling a membrane under free vibration can be stated as: Find u and λ, such that

$$\left\{ \begin{array}{rcll} -\mathrm{div}(\alpha \nabla u) & = & \lambda \rho u & \text{in} \quad \Omega, \\ u & = & 0 & \text{on} \quad \partial\Omega, \end{array} \right. \tag{5.6}$$

so that u represents the transverse displacement field, α is the stiffness coefficient and ρ is the density.

The associated first eigenvalue is defined as

$$\lambda_1 = \frac{\int_\Omega \alpha \|\nabla u\|^2}{\int_\Omega \rho |u|^2}, \tag{5.7}$$

with u solution of (5.6). The topological derivative for simple eigenvalues of the Laplacian can be found in Ammari and Khelifi (2003). The extension to multiple eigenvalues and other types of singular domain perturbations has been derived in Nazarov and Sokołowski (2008). In particular, the topological derivative of

$$\mathcal{F}(u) = \lambda_1^{-1} \tag{5.8}$$

is given by:

$$D_T \mathcal{F} = \frac{2\alpha \mathbf{P}_\alpha \nabla u \cdot \nabla u - (1-\gamma_\rho)\rho\lambda_1 |u|^2}{\lambda_1^2 \int_\Omega \rho |u|^2}, \tag{5.9}$$

which can be formally derived from Theorems 1 and 2. The rigorous justification for this result can be found in the book by (Novotny and Sokołowski, 2013, Ch 9). As observed by Haftka and Gürdal (1992), standard sensitivities of eigenvalues hold only in the case of distinct eigenvalues. According to Seyranian et al. (1994) symmetric and complex structures that depend on many design parameters often present multiple eigenvalues. A numerical method of solution was developed by the authors to determine an ascent direction in the design space for the smallest eigenvalue. More recently, a simple strategy proposed by Zhang et al. (2015) can be used in order to deal with multiplicity of eigenmodes, which consists in select the closest eigenmode to the current one. See also the paper by Torii and Rocha de Faria (2017) for more sophisticated approach based on a smooth p-norm approximation for the smallest eigenvalue.

6. Numerical Results

Let us introduce a hold-all domain $\mathcal{D} \subset \mathbb{R}^2$, such that $\Omega \subset \mathcal{D}$. By using the linear penalty method for volume control, the optimization problem we wish to solve is stated as follows:

$$\underset{\Omega \subset \mathcal{D}}{\text{Minimize}}\ \mathcal{F}_\Omega(u) = \mathcal{F}(u) + \mu|\Omega| \ , \tag{6.1}$$

subject to (5.1) or (5.6), where $\mu > 0$ is a user-defined multiplier. In particular, the shape function $\mathcal{F}(u)$ is defined through (5.2) or (5.8) according to the application we are dealing with, whereas the term $\mu|\Omega|$ is used to impose a restriction on the volume of elastic material, that is, the higher is μ the lower is the final volume $|\Omega|$. Since the problem is linear, the topological derivative of (6.1) is given by,

$$D_T \mathcal{F}_\Omega = D_T \mathcal{F} - \mu. \tag{6.2}$$

For this problem the topological derivative provides the descent direction of the shape functional and, consequently, leads to the solution of the problem. A topology optimization

algorithm based on the topological derivative and a level-set domain representation method is applied. It has been proposed by Amstutz and Andrä (2006) and consists basically in looking for a local optimality condition for the optimization problem (6.1), written in terms of the topological derivative and a level-set function (Amstutz, 2011). For more details, see the review paper by Novotny et al. (2019b). In particular, two stopping criteria are considered in the present algorithm: $\theta < 1^{\circ}$, which is the angle between the level-set function and the topological derivative, and $\kappa < 10^{-3}$, which represents the step size in the line-search process ($\kappa \in (0, 1]$). In this paper, the second stopping criterion has been reached in the Example 6.1 and the first stopping criterion has been reached in the Example 6.2. The hold-all domain is discretized by using linear triangular finite elements resulting in an initial uniform mesh with $160,000$ elements and $80,401$ nodes for the Example 6.1 and $6,400$ elements and $3,281$ nodes for the Example 6.2. In order to increase the accuracy as well as the topology smoothness four steps of mesh refinement during the iterative process are allowed. After the fourth refinement the resulting mesh presents $40,960,000$ elements and $20,486,401$ nodes for the Example 6.1 and $1,638,400$ elements and $820,481$ nodes for the Example 6.2.

6.1. **Heat exchange design.** The hold-all domain $\mathcal{D}$ is given by a unit square of size $(0, 1) \times (0, 1)$ with a distributed uniform heat generation of intensity $f = 10^4\, W$ over the domain. All the (Γ_N) boundary are thermally insulated, with exception of the region Γ_D of length 0.2. The temperature at Γ_D is prescribed as $u = 273\, K$. See sketch in Figure 1a. The penalty parameter is set as $\mu = 4$ and the weight as $\tau = 1$, whereas $\beta = 1$. During the optimization procedure two material are used, the first one is the aluminum ($\alpha = 205 W/mK$) and the second one is a material with low thermal conductivity $\gamma_\alpha \ll \alpha$. The initial domain consists of aluminum only ($\Omega = \mathcal{D}$). As the optimization process iterativelly evolves the aluminum is replaced by the second material. An external source producing a unidirectional wind flow with velocity V is also imposed to the problem. In order to evaluate the influence of the velocity profile on the final design a set of four cases are considered, as shown in Table 4.

TABLE 4. Example 1. Velocity and contrast.

	Case A	Case B	Case C	Case D
V	$(10, 0)$	$(-10, 0)$	$(0, 10)$	$(10, 0)$
γ_α	0.020	0.020	0.020	0.006

Figures 1b-c illustrate the intermediate topologies for Case A obtained at 10^{th} and 50^{th} iteration. The respective temperature fields are also presented in a 3D representation according to Figure 2. Based on these 3D colormaps it is possible to see how the device drains energy from all parts of the domain. Similar results, in absence of external source produced by wind flow, can be found in the literature (Bendsøe and Sigmund, 2003; Giusti et al., 2010). A comparison between the final topologies due to the different velocity profiles imposed to the problem can be seen in Figure 3 for the Cases A, B, C and D.

An analysis of the resulting topologies for each case allows us to observe the influence of the flow direction on the heat transfer over the domain. As the velocity vector changes the direction, final design is affected resulting in a complex geometry tending to a very refined root shape. A similar problem was also solved by Ikonen et al. (2018) using the L-Systems-based method but it failed to fine-tune the details of these designs as it did not use the gradient information of the objective function. A special attention must be given to Cases A and D, since they have the same wind flow velocity but with different γ_α, leading to different final designs.

The evolution histories for the shape functional and the volume fraction are presented in Figure 4. Cases A, B and C present similar behaviors as the iterative process evolve. The parameter γ_α was set the same for these three cases. In this sense, the velocity is the only

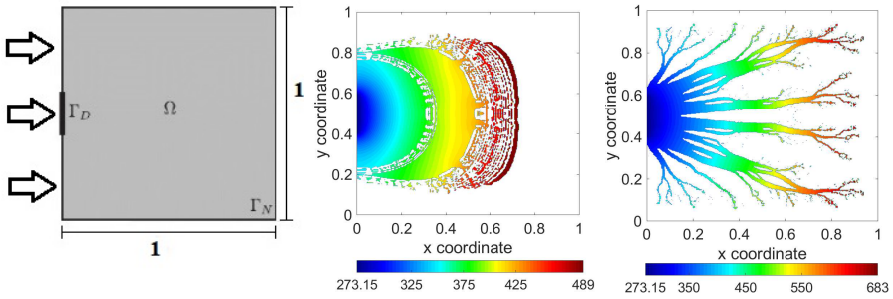

(a) initial domain (b) iteration $j = 10$ (c) iteration $j = 50$

FIGURE 1. Example 1. Initial domain and obtained topologies for Case A.

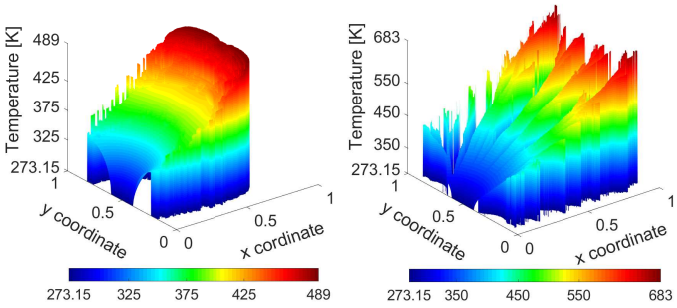

(a) iteration $j = 10$ (b) iteration $j = 50$

FIGURE 2. Example 1. Obtained temperature maps for Case A.

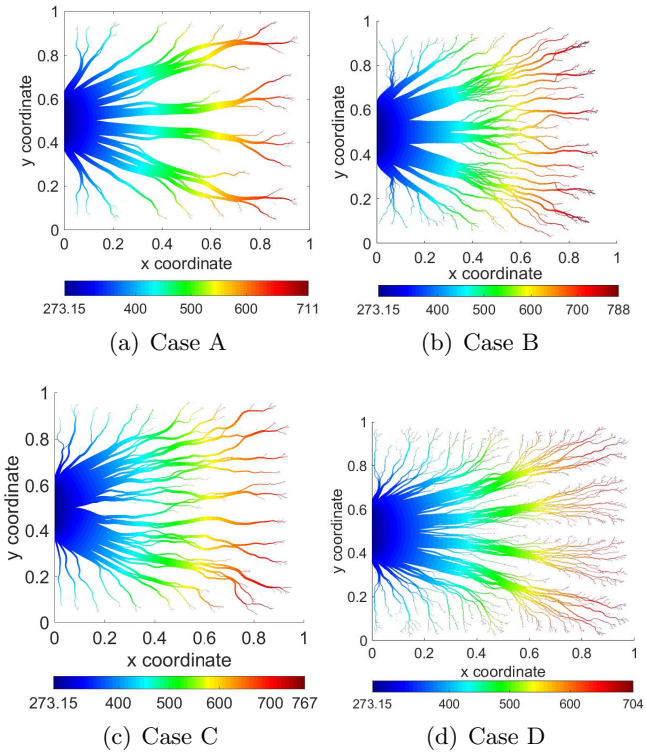

(a) Case A (b) Case B

(c) Case C (d) Case D

FIGURE 3. Example 1. Comparison of designs obtained for the representative Cases A, B, C and D.

variable driving the final resulting topologies for effect of comparison. In particular, the lack of horizontal symmetry observed in the obtained design for Case C can be explained by the vertical flow, which induces a kinking on the stream line of the heat flux. Case D presents a different behavior due to the lower value imposed to the parameter γ_α, consuming higher computational cost to reach the stopping criteria when compared to the previous cases.

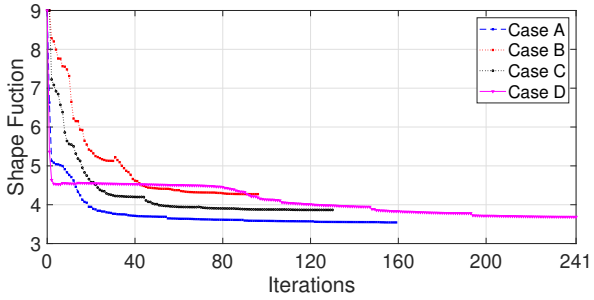

(a) shape functional

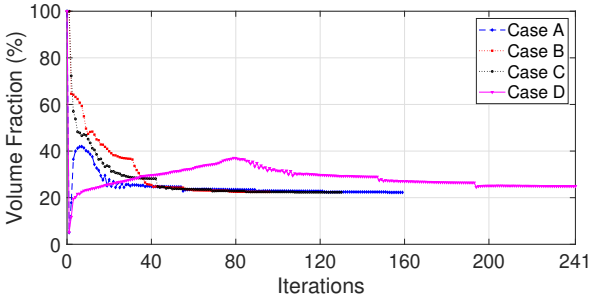

(b) volume fraction

FIGURE 4. Example 1. Shape functional and volume fraction.

6.2. **First eigenvalue maximization.** The hold-all domain $\mathcal{D}$ is given by a unit square membrane of size$(0,1) \times (0,1)$ with homogeneous Dirichlet boundary condition, contrast parameters $\gamma_\alpha = \gamma_\rho = 10^{-3}$ and non-structural concentrated mass of value 0.02 applied at the plate's center $(0.5, 0.5)$, as depicted in Figure 5a. The initial domain is set as $\Omega = \varnothing$. In order to evaluate the influence of the parameter μ on the final design a set of three cases are considered, as shown in Table 5.

TABLE 5. Example 2. Penalty parameter.

	Case A	Case B	Case C
μ	0.01	0.02	0.04

The final topologies for each case are presented in Figures 5b-d. Figure 6a shows the volume fraction history. Figures 6b-c present the first and second eigenvalues obtained during the iterative process. Note that they are completely separated, so that multiple eigenvalues phenomenon was not observed in this particular example. The first eigenvalue for the hold-all domain was calculated as $\lambda_1(\mathcal{D}) = 17.8993$ and depicted in Figure 6b (dashed-line). As the optimization process evolves the first eigenvalue obtained for each case investigated becomes comparable (Case C) and higher (Cases A and B) than the eigenvalue obtained for the non-designed domain. Finally, the first four intermediate topologies for Case B are shown in Figure 7, where we can observe that the concentrated mass acting at the center of the membrane is not connected with its boundary in the first two iterations, which explains the low value found for λ_1 at iterations $j = 1$ and $j = 2$.

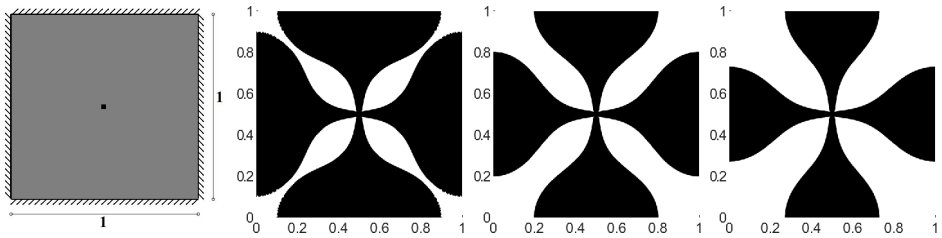

(a) hold-all domain (b) Case A (c) Case B (d) Case C

FIGURE 5. Example 2. Hold-all domain and optimized topologies for Cases A, B and C.

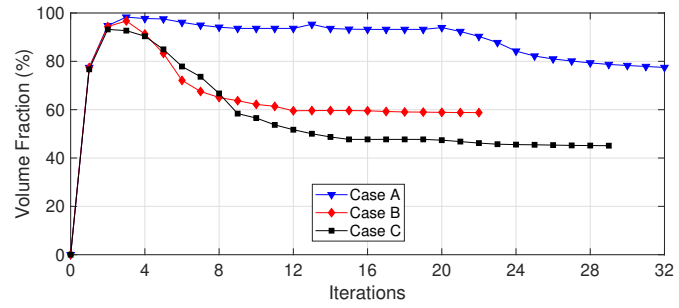

(a)

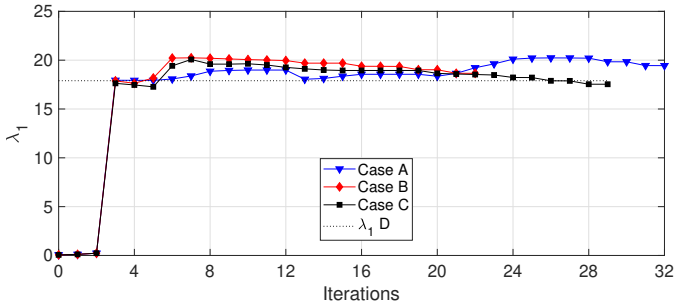

(b)

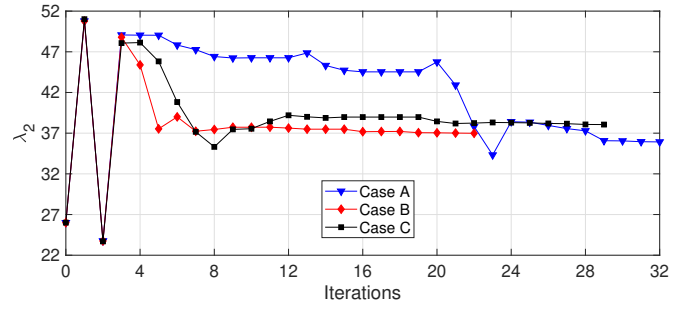

(c)

FIGURE 6. Example 2. (a) Volume fraction, (b) First eigenvalue $[\lambda_1]$ and (b) Second eigenvalue $[\lambda_2]$.

Finally, Table 6 summarizes the eigenvalues, shape functional values and final volume fraction obtained for each case, which are compared with the empty $\Omega = \varnothing$ and full $\Omega = \mathcal{D}$ domains counterparts. As it can be observed, the optimized membranes are much more efficient from the mechanical point of view than the non-optimized one for $\Omega = \mathcal{D}$,

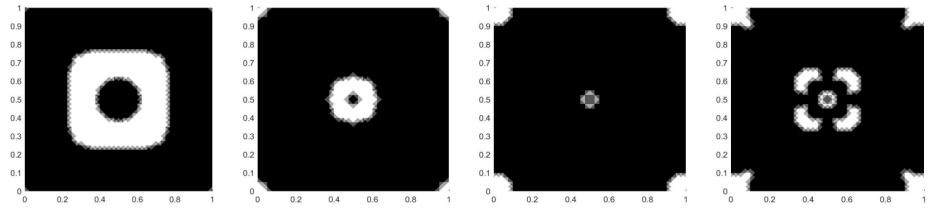

(a) iteration $j = 1$ (b) iteration $j = 2$ (c) iteration $j = 3$ (d) iteration $j = 4$

FIGURE 7. Example 2. First four intermediate topologies for Case B.

since less material is used to obtain comparable (Case C) and higher (Cases A and B) eigenvalues.

TABLE 6. Example 2. First eigenvalue, shape functional value and final volume fraction.

	Case A	Case B	Case C	$\Omega = \varnothing$	$\Omega = \mathcal{D}$
λ_1	19.1702	18.6080	17.5363	0.0623	17.8993
$\mathcal{F}_\Omega(u)$	0.0591	0.0653	0.0750	16.0418	0.0758
$\lvert\Omega\rvert$ (%)	77.4757	58.7762	45.1036	0.0000	100.00

7. Conclusions

In this paper, the topological asymptotic analysis of the L^2-norm and H^1-seminorm of the solution to a diffusive-convective-reactive problem, with respect to nucleation of inclusions endowed with different material properties of the background, has been considered. In particular, arguments on the existence of the topological derivative were given and estimation for the remainders left in the topological asymptotic expansion was rigorously derived. The resulting sensitivities were particularized for solving some selected problems, namely diffusive-convective energy dissipation minimization and membrane eigenvalue maximization. For the heat exchange model, the high efficiency material was progressively replaced by a low thermal conductive material until a complex design with high performance was achieved. Regarding the eigenvalue problem, the optimal design presented its first natural frequency maximized. In addition, an analysis was performed by comparison the first and second eigenvalues as the iterative process evolved. The multiple eigenvalue phenomena was not observed thus eliminating any presence of self-excited vibrations. The numerical experiments confirm the effectiveness of the proposed method.

Appendix A. Topological Asymptotic Analysis

Let us introduce an ansatz for the solution u_ε to the perturbed boundary value problem (3.5) of the form

$$u_\varepsilon(x) = u(x) + w_\varepsilon(x) + \widetilde{u}_\varepsilon(x), \tag{A.1}$$

where u is solution to the unperturbed boundary value problem (3.1), w_ε is solution to an exterior boundary value problem and $\widetilde{u}_\varepsilon$ is the remainder.

In particular, the exterior problem reads: Find w_ε, such that

$$\left\{\begin{array}{rcll} \operatorname{div}(\alpha_\varepsilon \nabla w_\varepsilon) & = & 0 & \text{in } \mathbb{R}^2\,, \\ w_\varepsilon & \to & 0 & \text{at } \infty \\ [\![w_\varepsilon]\!] & = & 0 \\ [\![\alpha_\varepsilon \nabla w_\varepsilon]\!] \cdot n & = & g \end{array}\right\} \text{ on } \partial B_\varepsilon\,, \tag{A.2}$$

where $g = (1 - \gamma_\alpha)\alpha \nabla u(\widehat{x}) \cdot n$. The solution to the exterior problem (A.2) is known in the literature because it has exactly the same structure as the Laplace boundary value

problem. In addition, for the particular case associated with circular inclusions, such solution is explicitly known (see for instance the paper by Ammari and Kang (2007)), namely

$$w_\varepsilon(x) = \mathbf{P}_\alpha \nabla u(\widehat{x}) \cdot (x - \widehat{x}) \quad \text{in} \quad B_\varepsilon, \tag{A.3}$$

$$w_\varepsilon(x) = \frac{\varepsilon^2}{\|x - \widehat{x}\|^2} \mathbf{P}_\alpha \nabla u(\widehat{x}) \cdot (x - \widehat{x}) \quad \text{in} \quad \mathbb{R}^2 \setminus B_\varepsilon. \tag{A.4}$$

Lemma 2. *Let w_ε be solution to the exterior problem* (A.2)*, then*

$$\|w_\varepsilon\|_{L^2(\Omega)} \leqslant C\varepsilon^2 \sqrt{|\ln(\varepsilon)|} = o(\varepsilon). \tag{A.5}$$

where constant C is independent of the small parameter ε.

Proof. It comes immediately from the explicit solutions (A.3) and (A.4). □

Finally, the remainder is constructed in order to compensate for the discrepancies introduced by the boundary layers w_ε and by the higher-order terms of the Taylor series expansion of ∇u around the point $\widehat{x} \in \Omega$. It means that $\widetilde{u}_\varepsilon$ has to be solution to the following boundary value problem: Find $\widetilde{u}_\varepsilon$, such that

$$\left\{ \begin{array}{rcll} -\mathrm{div}[\alpha_\varepsilon \nabla \widetilde{u}_\varepsilon(x) + \beta_\varepsilon(\nabla \widetilde{u}_\varepsilon \cdot V) + \rho_\varepsilon k \widetilde{u}_\varepsilon(x) & = & \beta_\varepsilon(\nabla w_\varepsilon \cdot V) + \rho_\varepsilon k w_\varepsilon & \text{in } \Omega, \\ \widetilde{u}_\varepsilon & = & \varepsilon^2 g_1 & \text{on } \partial\Omega, \\ [\![\widetilde{u}_\varepsilon]\!] & = & 0 \\ [\![\alpha_\varepsilon \nabla \widetilde{u}_\varepsilon]\!] n & = & \varepsilon g_2 & \text{on } \partial B_\varepsilon, \end{array} \right. \tag{A.6}$$

with functions $g_1 = -\varepsilon^{-2} w_\varepsilon$ and $g_2 = (1 - \gamma_\alpha)\alpha[\nabla^2 u(y)]n \cdot n$ independent of ε.

Lemma 3. *Let $\widetilde{u}_\varepsilon$ be solution of* (A.6) *or equivalently solution of the following variational problem*

$$\widetilde{u}_\varepsilon \in \widetilde{\mathcal{U}}_\varepsilon : \int_\Omega \alpha_\varepsilon \nabla \widetilde{u}_\varepsilon \cdot \nabla \eta + \int_\Omega \rho_\varepsilon k \widetilde{u}_\varepsilon \eta + \int_\Omega \beta_\varepsilon (\nabla \widetilde{u}_\varepsilon \cdot V)\eta$$
$$= \int_\Omega \beta_\varepsilon (\nabla w_\varepsilon \cdot V)\eta + \int_\Omega \rho_\varepsilon k w_\varepsilon \eta + \varepsilon \int_{\partial B_\varepsilon} g_2 \eta, \quad \forall \eta \in H_0^1(\Omega), \tag{A.7}$$

where the set $\widetilde{\mathcal{U}}_\varepsilon := \{\varphi \in H^1(\Omega) : \varphi_{|\partial\Omega} = \varepsilon^2 g_1\}$. Then, the estimate $\|\widetilde{u}_\varepsilon\|_{H^1(\Omega)} = o(\varepsilon)$ holds true.

Proof. By setting $\eta = \widetilde{u}_\varepsilon - \varphi_\varepsilon \in H_0^1(\Omega)$ as test function in (A.7), where $\varphi_\varepsilon \in \widetilde{\mathcal{U}}_\varepsilon$ is the lifting of the Dirichlet data $\varepsilon^2 g_1$ on $\partial\Omega$, we have

$$\int_\Omega \alpha_\varepsilon \|\nabla \widetilde{u}_\varepsilon\|^2 + \int_\Omega \rho_\varepsilon k |\widetilde{u}_\varepsilon|^2 = \underbrace{\varepsilon^2 \int_{\partial\Omega} g_1 \alpha \partial_n \widetilde{u}_\varepsilon}_{E_1} + \underbrace{\varepsilon \int_{\partial B_\varepsilon} g_2 \widetilde{u}_\varepsilon}_{E_2}$$
$$+ \underbrace{\int_\Omega \beta_\varepsilon (\nabla \widetilde{u}_\varepsilon \cdot V) w_\varepsilon}_{E_3} - \underbrace{\int_\Omega \rho_\varepsilon k w_\varepsilon \widetilde{u}_\varepsilon}_{E_4}. \tag{A.8}$$

since

$$\int_\Omega \beta_\varepsilon (\nabla w_\varepsilon \cdot V)\widetilde{u}_\varepsilon = -\int_\Omega \beta_\varepsilon (\nabla \widetilde{u}_\varepsilon \cdot V) w_\varepsilon. \tag{A.9}$$

Therefore, from the Cauchy-Schwarz inequality there are

$$|E_1| = \varepsilon^2 \left| \int_{\partial\Omega} g_1 \alpha \partial_n \widetilde{u}_\varepsilon \right| \leqslant \varepsilon^2 \|g_1\|_{L^2(\partial\Omega)} \|\partial_n \widetilde{u}_\varepsilon\|_{L^2(\partial\Omega)} \leqslant C_1 \varepsilon^2 \|\widetilde{u}_\varepsilon\|_{H^1(\Omega)}, \tag{A.10}$$

$$|E_2| = \varepsilon \left| \int_{\partial B_\varepsilon} g_2 \widetilde{u}_\varepsilon \right| \leqslant \varepsilon \|g_2\|_{L^2(\partial B_\varepsilon)} \|\widetilde{u}_\varepsilon\|_{L^2(\partial B_\varepsilon)} \leqslant C_2 \varepsilon^{3/2} \|\widetilde{u}_\varepsilon\|_{H^1(\Omega)}, \tag{A.11}$$

$$|E_3| = \left| \int_\Omega \beta_\varepsilon (\nabla \widetilde{u}_\varepsilon \cdot V) w_\varepsilon \right| \leqslant \|\nabla \widetilde{u}_\varepsilon\|_{L^2(\Omega)} \|w_\varepsilon\|_{L^2(\Omega)} \leqslant C_3 \varepsilon^2 \sqrt{|\ln(\varepsilon)|} \|\widetilde{u}_\varepsilon\|_{H^1(\Omega)}, \tag{A.12}$$

$$|E_4| = \left| \int_\Omega \rho_\varepsilon k w_\varepsilon \widetilde{u}_\varepsilon \right| \leqslant \|w_\varepsilon\|_{L^2(\Omega)} \|\widetilde{u}_\varepsilon\|_{L^2(\Omega)} \leqslant C_4 \varepsilon^2 \sqrt{|\ln(\varepsilon)|} \|\widetilde{u}_\varepsilon\|_{H^1(\Omega)}, \tag{A.13}$$

where we have used Lemma 2. From these last results, we obtain

$$\int_\Omega \rho_\varepsilon \|\nabla \widetilde{u}_\varepsilon\|^2 + \int_\Omega \rho_\varepsilon k |\widetilde{u}_\varepsilon|^2 \leqslant C_5 (\varepsilon^2 + \varepsilon^{3/2} + \varepsilon^2 \sqrt{|\ln(\varepsilon)|}) \|\widetilde{u}_\varepsilon\|_{H^1(\Omega)}. \tag{A.14}$$

By taking into account the coercivity of the bilinear form on the left-hand side of the above inequality, there is

$$c \|\widetilde{u}_\varepsilon\|^2_{H^1(\Omega)} \leqslant \int_\Omega \rho_\varepsilon \|\nabla \widetilde{u}_\varepsilon\|^2 + \int_\Omega \rho_\varepsilon k |\widetilde{u}_\varepsilon|^2, \tag{A.15}$$

which leads to the result with constants c and C_5 independent of ε. □

Corollary 1. *Let u and u_ε be solutions of problems* (3.1) *and* (3.5)*, respectively. Then*

$$\|u_\varepsilon - u\|_{L^2(\Omega)} = o(\varepsilon). \tag{A.16}$$

Proof. By taking into account the ansatz (A.1) and the triangular inequality, it follows that

$$\begin{aligned} \|u_\varepsilon - u\|_{L^2(\Omega)} &= \|w_\varepsilon + \widetilde{u}_\varepsilon\|_{L^2(\Omega)} \\ &\leqslant \|w_\varepsilon\|_{L^2(\Omega)} + \|\widetilde{u}_\varepsilon\|_{L^2(\Omega)} \\ &\leqslant \|w_\varepsilon\|_{L^2(\Omega)} + \|\widetilde{u}_\varepsilon\|_{H^1(\Omega)} = o(\varepsilon). \end{aligned} \tag{A.17}$$

where we have used Lemmas 2 and 3. □

Before proceed, let us subtract (3.1) from (3.5). After a simple manipulation by taking into account the contrasts (Tables 2 and 3), one can obtain

$$\begin{aligned} \int_\Omega \alpha \nabla(u_\varepsilon - u) \cdot \nabla \eta + \int_\Omega \beta (\nabla(u_\varepsilon - u) \cdot V) \eta + \int_\Omega \rho k (u_\varepsilon - u) \eta \\ = \int_{B_\varepsilon} (1 - \gamma_\alpha) \alpha \nabla u_\varepsilon \cdot \nabla \eta + \int_{B_\varepsilon} (1 - \gamma_\beta) \beta (\nabla u_\varepsilon \cdot V) \eta \\ + \int_{B_\varepsilon} (1 - \gamma_\rho) \rho k u_\varepsilon \eta - \int_{B_\varepsilon} (1 - \gamma_f) f \eta. \end{aligned} \tag{A.18}$$

A.1. **Proof of Theorem 1.** By subtracting $\mathcal{G}(u)$ from $\mathcal{G}_\varepsilon(u_\varepsilon)$, there is

$$\mathcal{G}_\varepsilon(u_\varepsilon) - \mathcal{G}(u) = \underbrace{2 \int_\Omega \rho k (u_\varepsilon - u) u}_{A_1} \underbrace{- \int_{B_\varepsilon} (1 - \gamma_\rho) \rho k |u_\varepsilon|^2}_{A_2} + \underbrace{\int_\Omega \rho k |u_\varepsilon - u|^2}_{\mathcal{E}_1(\varepsilon)}, \tag{A.19}$$

with remainder $\mathcal{E}_1(\varepsilon)$ bounded as follows

$$|\mathcal{E}_1(\varepsilon)| \leqslant C_1 \|u_\varepsilon - u\|^2_{L^2(\Omega)} = o(\varepsilon^2), \tag{A.20}$$

where we have used Corollary 1. The integral A_2 can be trivially expanded as follows

$$A_2 = \pi\varepsilon^2(1-\gamma_\rho)\rho k|u|^2(\widehat{x}) + \underbrace{\int_{B_\varepsilon}(1-\gamma_\rho)\rho k|u_\varepsilon - u|^2}_{\mathcal{E}_2(\varepsilon)} + \underbrace{2\int_{B_\varepsilon}(1-\gamma_\rho)\rho k(u_\varepsilon - u)u}_{\mathcal{E}_3(\varepsilon)} + \underbrace{\int_{B_\varepsilon}(1-\gamma_\rho)\rho k[|u|^2 - |u(\widehat{x})|^2]}_{\mathcal{E}_4(\varepsilon)}. \quad (A.21)$$

with remainders $\mathcal{E}_2(\varepsilon)$, $\mathcal{E}_3(\varepsilon)$ and $\mathcal{E}_4(\varepsilon)$ bounded as follows

$$|\mathcal{E}_2(\varepsilon)| \leqslant C_2\|u_\varepsilon - u\|^2_{L^2(\Omega)} = o(\varepsilon^2), \quad (A.22)$$

$$|\mathcal{E}_3(\varepsilon)| \leqslant C_3\varepsilon\|u_\varepsilon - u\|_{L^2(\Omega)} = o(\varepsilon^2), \quad (A.23)$$

$$|\mathcal{E}_4(\varepsilon)| \leqslant C_4\|x - \widehat{x}\|^2_{L^2(B_\varepsilon)} = o(\varepsilon^2). \quad (A.24)$$

where we have used Corollary 1 together with the interior elliptic regularity of function u. Now, let us set $\eta = q$ in (A.18) and $\eta = u_\varepsilon - u$ in the adjoint equation (3.3). After comparing the obtained results, the integral A_1 can be rewritten as

$$A_1 = -\underbrace{\int_{B_\varepsilon}(1-\gamma_\alpha)\alpha\nabla u_\varepsilon\cdot\nabla q}_{A_3} - \underbrace{\int_{B_\varepsilon}(1-\gamma_\beta)\beta(\nabla u_\varepsilon\cdot V)q}_{A_4} - \underbrace{\int_{B_\varepsilon}(1-\gamma_\rho)\rho k u_\varepsilon q}_{A_5} + \underbrace{\int_{B_\varepsilon}(1-\gamma_f)fq}_{A_6}. \quad (A.25)$$

The integrals A_5 and A_6 are trivially expanded as

$$A_5 = \pi\varepsilon^2(1-\gamma_\rho)\rho k u q(\widehat{x}) + \underbrace{\int_{B_\varepsilon}(1-\gamma_\rho)\rho k(u_\varepsilon - u)q}_{\mathcal{E}_5(\varepsilon)} + \underbrace{\int_{B_\varepsilon}(1-\gamma_\rho)\rho k[uq - uq(\widehat{x})]}_{\mathcal{E}_6(\varepsilon)}, \quad (A.26)$$

$$A_6 = \pi\varepsilon^2(1-\gamma_f)fq(\widehat{x}) + \underbrace{\int_{B_\varepsilon}(1-\gamma_f)f[q - q(\widehat{x})]}_{\mathcal{E}_7(\varepsilon)}. \quad (A.27)$$

with remainder $\mathcal{E}_5(\varepsilon)$, $\mathcal{E}_6(\varepsilon)$ and $\mathcal{E}_7(\varepsilon)$ bounded as follows

$$|\mathcal{E}_5(\varepsilon)| \leqslant \varepsilon\|u_\varepsilon - u\|_{L^2(\Omega)} = o(\varepsilon^2), \quad (A.28)$$

$$|\mathcal{E}_6(\varepsilon)| \leqslant \varepsilon\|x - \widehat{x}\|_{L^2(B_\varepsilon)} = o(\varepsilon^2), \quad (A.29)$$

$$|\mathcal{E}_7(\varepsilon)| \leqslant \varepsilon\|x - \widehat{x}\|_{L^2(B_\varepsilon)} = o(\varepsilon^2), \quad (A.30)$$

where we have used Corollary 1 and the interior elliptic regularity of functions u and q. The integrals A_3 and A_4 can be developed in the following way,

$$A_3 + A_4 = \underbrace{\int_{B_\varepsilon}(1-\gamma_\alpha)\alpha\nabla u\cdot\nabla q}_{A_7} + \underbrace{\int_{B_\varepsilon}(1-\gamma_\alpha)\alpha\nabla w_\varepsilon\cdot\nabla q}_{A_8} + \underbrace{\int_{B_\varepsilon}(1-\gamma_\alpha)\alpha\nabla\widetilde{u}_\varepsilon\cdot\nabla q}_{\mathcal{E}_8(\varepsilon)} + \underbrace{\int_{B_\varepsilon}(1-\gamma_\beta)\beta(\nabla u\cdot V)q}_{A_9} + \underbrace{\int_{B_\varepsilon}(1-\gamma_\beta)\beta(\nabla w_\varepsilon\cdot V)q}_{A_{10}} + \underbrace{\int_{B_\varepsilon}(1-\gamma_\beta)\beta(\nabla\widetilde{u}_\varepsilon\cdot V)q}_{\mathcal{E}_9(\varepsilon)}, \quad (A.31)$$

where we have introduced the ansatz (A.1). Therefore,

$$A_7 = \pi\varepsilon^2(1-\gamma_\alpha)\alpha\nabla u\cdot\nabla q(\widehat{x}) + \underbrace{\int_{B_\varepsilon}(1-\gamma_\alpha)\alpha[\nabla u\cdot\nabla q - \nabla u\cdot\nabla q(\widehat{x})]}_{\mathcal{E}_{10}(\varepsilon)}, \tag{A.32}$$

$$A_9 = \pi\varepsilon^2(1-\gamma_\beta)\beta(\nabla u\cdot V)q(\widehat{x}) + \underbrace{\int_{B_\varepsilon}(1-\gamma_\beta)\beta[(\nabla u\cdot V)q - (\nabla u\cdot V)q(\widehat{x})]}_{\mathcal{E}_{11}(\varepsilon)} \tag{A.33}$$

with remainders $\mathcal{E}_8(\varepsilon)$, $\mathcal{E}_9(\varepsilon)$, $\mathcal{E}_{10}(\varepsilon)$ and $\mathcal{E}_{11}(\varepsilon)$ bounded as follows

$$|\mathcal{E}_8(\varepsilon)| \leqslant \varepsilon\|\widetilde{u}_\varepsilon\|_{H^1(\Omega)} = o(\varepsilon^2), \tag{A.34}$$

$$|\mathcal{E}_9(\varepsilon)| \leqslant \varepsilon\|\widetilde{u}_\varepsilon\|_{H^1(\Omega)} = o(\varepsilon^2), \tag{A.35}$$

$$|\mathcal{E}_{10}(\varepsilon)| \leqslant \varepsilon\|x-\widehat{x}\|_{L^2(B_\varepsilon)} = o(\varepsilon^2), \tag{A.36}$$

$$|\mathcal{E}_{11}(\varepsilon)| \leqslant \varepsilon\|x-\widehat{x}\|_{L^2(B_\varepsilon)} = o(\varepsilon^2), \tag{A.37}$$

where we have used Lemma 3 together with the interior elliptic regularity of functions u and q. The last two integrals A_8 and A_{10} can be rewritten as

$$A_8 = \pi\varepsilon^2(1-\gamma_\alpha)\alpha\mathbf{P}_\alpha\nabla u\cdot\nabla q(\widehat{x}) + \underbrace{\int_{B_\varepsilon}(1-\gamma_\alpha)\alpha\nabla w_\varepsilon\cdot\nabla(q-q(\widehat{x}))}_{\mathcal{E}_{12}(\varepsilon)}, \tag{A.38}$$

$$A_{10} = \pi\varepsilon^2(1-\gamma_\beta)\beta(\mathbf{P}_{\alpha\beta}\nabla u\cdot V)q(\widehat{x}) + \underbrace{\int_{B_\varepsilon}(1-\gamma_\beta)\beta(\nabla w_\varepsilon\cdot V)(q-q(\widehat{x}))}_{\mathcal{E}_{13}(\varepsilon)}, \tag{A.39}$$

where we have used the explicit solution (A.4). The remainders $\mathcal{E}_{12}(\varepsilon)$ and $\mathcal{E}_{13}(\varepsilon)$ can be bounded as follows

$$|\mathcal{E}_{12}(\varepsilon)| \leqslant C_5\|\nabla w_\varepsilon\|_{L^2(B_\varepsilon)}\|x-\widehat{x}\|_{L^2(B_\varepsilon)} = o(\varepsilon^2), \tag{A.40}$$

$$|\mathcal{E}_{13}(\varepsilon)| \leqslant C_6\|\nabla w_\varepsilon\|_{L^2(B_\varepsilon)}\|x-\widehat{x}\|_{L^2(B_\varepsilon)} = o(\varepsilon^2). \tag{A.41}$$

Finally, after collecting the obtained results, we have

$$\begin{aligned}\mathcal{G}_\varepsilon(u_\varepsilon) - \mathcal{G}(u) = -\pi\varepsilon^2[&2\alpha\mathbf{P}_\alpha\nabla u\cdot\nabla q(\widehat{x}) + 2\beta(\mathbf{P}_{\alpha\beta}\nabla u\cdot V)q(\widehat{x}) \\ &+ (1-\gamma_\rho)\rho k u(u+q)(\widehat{x}) - (1-\gamma_f)fq(\widehat{x})] + \sum_{i=1}^{13}\mathcal{E}_i(\varepsilon),\end{aligned} \tag{A.42}$$

where the remainders $\mathcal{E}_i(\varepsilon) = o(\varepsilon^2)$, for $i = 1\cdots 13$.

A.2. **Proof of Theorem 2.** Let us subtract $\mathcal{J}(u)$ from $\mathcal{J}_\varepsilon(u_\varepsilon)$, to obtain

$$\mathcal{J}_\varepsilon(u_\varepsilon) - \mathcal{J}(u) = 2\int_\Omega \alpha\nabla(u_\varepsilon - u)\cdot\nabla u - \int_{B_\varepsilon}(1-\gamma_\alpha)\alpha\|\nabla u_\varepsilon\|^2 + \underbrace{\int_\Omega \alpha\|\nabla(u_\varepsilon-u)\|^2}_{B_1}. \tag{A.43}$$

By setting $\eta = u_\varepsilon - u$ as test function in (A.18), the integral B_1 can be rewritten, after some manipulations, as

$$B_1 = \int_{B_\varepsilon}(1-\gamma_\alpha)\alpha\nabla u_\varepsilon\cdot\nabla(u_\varepsilon - u) + \mathcal{E}_{14}(\varepsilon). \tag{A.44}$$

The remainder $\mathcal{E}_{14}(\varepsilon)$ is defined as

$$\begin{aligned}\mathcal{E}_{14}(\varepsilon) = &\int_{B_\varepsilon}(1-\gamma_\beta)\beta(\nabla(u_\varepsilon-u)\cdot V)(u_\varepsilon-u)+\int_{B_\varepsilon}(1-\gamma_\beta)\beta(\nabla u\cdot V)(u_\varepsilon-u)\\ &+\int_{B_\varepsilon}(1-\gamma_\rho)\rho k|u_\varepsilon-u|^2+\int_{B_\varepsilon}(1-\gamma_\rho)\rho k u(u_\varepsilon-u)-\int_{B_\varepsilon}(1-\gamma_f)f(u_\varepsilon-u)\\ &-\int_\Omega\beta(\nabla(u_\varepsilon-u)\cdot V)(u_\varepsilon-u)-\int_\Omega\rho k|u_\varepsilon-u|^2, \quad \text{(A.45)}\end{aligned}$$

which can be bounded as follow

$$\begin{aligned}|\mathcal{E}_{14}(\varepsilon)| &\leqslant C_1(\varepsilon+\|u_\varepsilon-u\|_{L^2(B_\varepsilon)}+\|\nabla(u_\varepsilon-u)\|_{L^2(B_\varepsilon)})\|u_\varepsilon-u\|_{L^2(B_\varepsilon)}\\ &+ C_2(\|u_\varepsilon-u\|_{L^2(\Omega)}+\|\nabla(u_\varepsilon-u)\|_{L^2(\Omega)})\|u_\varepsilon-u\|_{L^2(\Omega)}\\ &\leqslant C_3\|u_\varepsilon-u\|_{L^2(\Omega)}\|u_\varepsilon-u\|_{H^1(\Omega)}=o(\varepsilon^2), \quad \text{(A.46)}\end{aligned}$$

where we have used the Cauchy-Schwarz inequality together with Lemma 1 and Corollary 1. Therefore, equation (A.43) becomes

$$\mathcal{J}_\varepsilon(u_\varepsilon)-\mathcal{J}(u)=\underbrace{2\int_\Omega\alpha\nabla(u_\varepsilon-u)\cdot\nabla u}_{B_2}-\underbrace{\int_{B_\varepsilon}(1-\gamma_\alpha)\alpha\nabla u_\varepsilon\cdot\nabla u}_{B_3}+\mathcal{E}_{14}(\varepsilon). \quad \text{(A.47)}$$

From the ansatz (A.1), integral B_3 can be written as

$$B_3=\underbrace{\int_{B_\varepsilon}(1-\gamma_\alpha)\alpha\|\nabla u\|^2}_{B_4}+\underbrace{\int_{B_\varepsilon}(1-\gamma_\alpha)\alpha\nabla w_\varepsilon\cdot\nabla u}_{B_5}+\underbrace{\int_{B_\varepsilon}(1-\gamma_\alpha)\alpha\nabla u\cdot\nabla\widetilde{u}_\varepsilon}_{\mathcal{E}_{15}(\varepsilon)}, \quad \text{(A.48)}$$

with the remainder $\mathcal{E}_{15}(\varepsilon)$ bounded as follows

$$|\mathcal{E}_{15}(\varepsilon)|\leqslant C_1\varepsilon\|\nabla\widetilde{u}_\varepsilon\|_{L^2(B_\varepsilon)}\leqslant C_2\varepsilon\|\widetilde{u}_\varepsilon\|_{H^1(\Omega)}=o(\varepsilon^2) \quad \text{(A.49)}$$

where we have used Lemma 3. The integrals B_4 and B_5 can be trivially expanded as follows

$$B_4 = \pi\varepsilon^2(1-\gamma_\alpha)\alpha\|\nabla u(\widehat{x})\|^2+\underbrace{\int_{B_\varepsilon}(1-\gamma_\alpha)\alpha(\|\nabla u\|^2-\|\nabla u(\widehat{x})\|^2)}_{\mathcal{E}_{16}(\varepsilon)}, \quad \text{(A.50)}$$

$$B_5 = \pi\varepsilon^2(1-\gamma_\alpha)\alpha\mathbf{P}_\alpha\nabla u\cdot\nabla u(\widehat{x})+\underbrace{\int_{B_\varepsilon}(1-\gamma_\alpha)\alpha\nabla w_\varepsilon\cdot(\nabla u-\nabla u(\widehat{x}))}_{\mathcal{E}_{17}(\varepsilon)}, \quad \text{(A.51)}$$

where we have used the explicit solution (A.4). The remainders $\mathcal{E}_{16}(\varepsilon)$ and $\mathcal{E}_{17}(\varepsilon)$ can be bounded as follows

$$\begin{aligned}|\mathcal{E}_{16}(\varepsilon)| &\leqslant C_1\varepsilon\|x-\widehat{x}\|_{L^2(B_\varepsilon)}=o(\varepsilon^2), \quad \text{(A.52)}\\ |\mathcal{E}_{17}(\varepsilon)| &\leqslant C_2\|\nabla w_\varepsilon\|_{L^2(B_\varepsilon)}\|x-\widehat{x}\|_{L^2(B_\varepsilon)}=o(\varepsilon^2). \quad \text{(A.53)}\end{aligned}$$

Now, let us set $\eta=p$ in (A.18) and $\eta=u_\varepsilon-u$ in the adjoint equation (3.4). After comparing the obtained results, the integral B_2 can be rewritten as

$$\begin{aligned}B_2=&-\underbrace{\int_{B_\varepsilon}(1-\gamma_\alpha)\alpha\nabla u_\varepsilon\cdot\nabla p}_{B_6}-\underbrace{\int_{B_\varepsilon}(1-\gamma_\beta)\beta(\nabla u_\varepsilon\cdot V)p}_{B_7}\\ &-\underbrace{\int_{B_\varepsilon}(1-\gamma_\rho)\rho k u_\varepsilon p}_{B_8}+\underbrace{\int_{B_\varepsilon}(1-\gamma_f)fp}_{B_9}. \quad \text{(A.54)}\end{aligned}$$

The integrals B_8 and B_9 are trivially expanded as

$$B_8 = \pi\varepsilon^2(1-\gamma_\rho)\rho k u p(\widehat{x}) + \underbrace{\int_{B_\varepsilon}(1-\gamma_\rho)\rho k(u_\varepsilon - u)p}_{\mathcal{E}_{18}(\varepsilon)} + \underbrace{\int_{B_\varepsilon}(1-\gamma_\rho)\rho k[up - up(\widehat{x})]}_{\mathcal{E}_{19}(\varepsilon)}, \quad \text{(A.55)}$$

$$B_9 = \pi\varepsilon^2(1-\gamma_f) f p(\widehat{x}) + \underbrace{\int_{B_\varepsilon}(1-\gamma_f) f[p - p(\widehat{x})]}_{\mathcal{E}_{20}(\varepsilon)}. \quad \text{(A.56)}$$

with remainder $\mathcal{E}_{18}(\varepsilon)$, $\mathcal{E}_{19}(\varepsilon)$ and $\mathcal{E}_{20}(\varepsilon)$ bounded as follows

$$|\mathcal{E}_{18}(\varepsilon)| \leqslant \varepsilon\|u_\varepsilon - u\|_{L^2(\Omega)} = o(\varepsilon^2), \quad \text{(A.57)}$$

$$|\mathcal{E}_{19}(\varepsilon)| \leqslant \varepsilon\|x - \widehat{x}\|_{L^2(B_\varepsilon)} = o(\varepsilon^2), \quad \text{(A.58)}$$

$$|\mathcal{E}_{20}(\varepsilon)| \leqslant \varepsilon\|x - \widehat{x}\|_{L^2(B_\varepsilon)} = o(\varepsilon^2), \quad \text{(A.59)}$$

where we have used Corollary 1 and the interior elliptic regularity of functions u and p. The integrals B_6 and B_7 can be developed in the following way,

$$\begin{aligned} B_6 + B_7 = &\underbrace{\int_{B_\varepsilon}(1-\gamma_\alpha)\alpha\nabla u\cdot\nabla p}_{B_{10}} + \underbrace{\int_{B_\varepsilon}(1-\gamma_\alpha)\alpha\nabla w_\varepsilon\cdot\nabla p}_{B_{11}} \\ &+ \underbrace{\int_{B_\varepsilon}(1-\gamma_\alpha)\alpha\nabla\widetilde{u}_\varepsilon\cdot\nabla p}_{\mathcal{E}_{21}(\varepsilon)} + \underbrace{\int_{B_\varepsilon}(1-\gamma_\beta)\beta(\nabla u\cdot V)p}_{B_{12}} \\ &+ \underbrace{\int_{B_\varepsilon}(1-\gamma_\beta)\beta(\nabla w_\varepsilon\cdot V)p}_{B_{13}} + \underbrace{\int_{B_\varepsilon}(1-\gamma_\beta)\beta(\nabla\widetilde{u}_\varepsilon\cdot V)p}_{\mathcal{E}_{22}(\varepsilon)}, \end{aligned} \quad \text{(A.60)}$$

where we have introduced the ansatz (A.1). Therefore,

$$B_{10} = \pi\varepsilon^2(1-\gamma_\alpha)\alpha\nabla u\cdot\nabla p(\widehat{x}) + \underbrace{\int_{B_\varepsilon}(1-\gamma_\alpha)\alpha[\nabla u\cdot\nabla p - \nabla u\cdot\nabla p(\widehat{x})]}_{\mathcal{E}_{23}(\varepsilon)}, \quad \text{(A.61)}$$

$$B_{12} = \pi\varepsilon^2(1-\gamma_\beta)\beta(\nabla u\cdot V)p(\widehat{x}) + \underbrace{\int_{B_\varepsilon}(1-\gamma_\beta)\beta[(\nabla u\cdot V)p - (\nabla u\cdot V)p(\widehat{x})]}_{\mathcal{E}_{24}(\varepsilon)}, \quad \text{(A.62)}$$

with remainders $\mathcal{E}_{21}(\varepsilon)$, $\mathcal{E}_{22}(\varepsilon)$, $\mathcal{E}_{23}(\varepsilon)$ and $\mathcal{E}_{24}(\varepsilon)$ bounded as follows

$$|\mathcal{E}_{21}(\varepsilon)| \leqslant \varepsilon\|\widetilde{u}_\varepsilon\|_{H^1(\Omega)} = o(\varepsilon^2), \quad \text{(A.63)}$$

$$|\mathcal{E}_{22}(\varepsilon)| \leqslant \varepsilon\|\widetilde{u}_\varepsilon\|_{H^1(\Omega)} = o(\varepsilon^2), \quad \text{(A.64)}$$

$$|\mathcal{E}_{23}(\varepsilon)| \leqslant \varepsilon\|x - \widehat{x}\|_{L^2(B_\varepsilon)} = o(\varepsilon^2), \quad \text{(A.65)}$$

$$|\mathcal{E}_{24}(\varepsilon)| \leqslant \varepsilon\|x - \widehat{x}\|_{L^2(B_\varepsilon)} = o(\varepsilon^2), \quad \text{(A.66)}$$

where we have used Lemma 3 together with the interior elliptic regularity of functions u and p. The last two integrals B_{11} and B_{13} can be rewritten as

$$B_{11} = \pi\varepsilon^2(1-\gamma_\alpha)\alpha\mathbf{P}_\alpha\nabla u\cdot\nabla p(\widehat{x}) + \underbrace{\int_{B_\varepsilon}(1-\gamma_\alpha)\alpha\nabla w_\varepsilon\cdot\nabla(p - p(\widehat{x}))}_{\mathcal{E}_{25}(\varepsilon)}, \quad \text{(A.67)}$$

$$B_{13} = \pi\varepsilon^2(1-\gamma_\beta)\beta(\mathbf{P}_\alpha\nabla u\cdot V)p(\widehat{x}) + \underbrace{\int_{B_\varepsilon}(1-\gamma_\beta)\beta(\nabla w_\varepsilon\cdot V)(p - p(\widehat{x}))}_{\mathcal{E}_{26}(\varepsilon)}, \quad \text{(A.68)}$$

where we have used the explicit solution (A.4). The remainders $\mathcal{E}_{25}(\varepsilon)$ and $\mathcal{E}_{26}(\varepsilon)$ can be bounded as follows

$$|\mathcal{E}_{25}(\varepsilon)| \leqslant C_1\|\nabla w_\varepsilon\|_{L^2(B_\varepsilon)}\|x-\widehat{x}\|_{L^2(B_\varepsilon)} = o(\varepsilon^2), \tag{A.69}$$

$$|\mathcal{E}_{26}(\varepsilon)| \leqslant C_2\|\nabla w_\varepsilon\|_{L^2(B_\varepsilon)}\|x-\widehat{x}\|_{L^2(B_\varepsilon)} = o(\varepsilon^2). \tag{A.70}$$

Finally, after collecting the obtained results, we have

$$\begin{aligned}\mathcal{J}_\varepsilon(u_\varepsilon) - \mathcal{J}(u) = -\pi\varepsilon^2[2\alpha\mathbf{P}_\alpha\nabla u\cdot\nabla(u+p)(\widehat{x}) + 2\beta(\mathbf{P}_{\alpha\beta}\nabla u\cdot V)p(\widehat{x}) \\ + (1-\gamma_\rho)\rho k u p(\widehat{x}) - (1-\gamma_f)fp(\widehat{x})] + \sum_{i=14}^{26}\mathcal{E}_i(\varepsilon),\end{aligned} \tag{A.71}$$

where the remainders $\mathcal{E}_i(\varepsilon) = o(\varepsilon^2)$, for $i = 14\cdots 26$.

References

H. Ammari and H. Kang. *Polarization and moment tensors with applications to inverse problems and effective medium theory.* Applied Mathematical Sciences vol. 162. Springer-Verlag, New York, 2007.

H. Ammari and A. Khelifi. Electromagnetic scattering by small dielectric inhomogeneities. *ournal de Mathématiques Pures et Appliquées*, 82:749–842, 2003.

H. Ammari, H. Kang, H. Lee, and J. Lim. Boundary perturbations due to the presence of small linear cracks in an elastic body. *Journal of Elasticity*, 113:75–91, 2013.

S. Amstutz. Analysis of a level set method for topology optimization. *Optimization Methods and Software*, 26(4-5):555–573, 2011.

S. Amstutz and H. Andrä. A new algorithm for topology optimization using a level-set method. *Journal of Computational Physics*, 216(2):573–588, 2006.

S. Amstutz, S. M. Giusti, A. A. Novotny, and E. A. de Souza Neto. Topological derivative for multi-scale linear elasticity models applied to the synthesis of microstructures. *International Journal for Numerical Methods in Engineering*, 84:733–756, 2010.

C. T. M. Anflor, K. L. Teotônio, and J. N. V. Goulart. Structural optimization using theboundary element method and topological derivative applied to a suspension trailing arm. *Engineering Optimization*, 50(10):1662–1680, 2018.

A. Bejan. Constructal-theory network of conducting paths for cooling a heat generating volume. *International Journal of Heat and Mass Transfer*, 40(4):799 – 816, 1997.

A. Bejan, G. Tsatsaronis, and M. Moran. *Thermal Design and Optimization.* Wiley-Interscience, New York, 1995.

M. P. Bendsøe and O. Sigmund. *Topology optimization. Theory, methods and applications.* Springer-Verlag, Berlin, 2003.

D. Bojczuk and Z. Mróz. Topological sensitivity derivative with respect to area, shape and orientation of an elliptic hole in a plate. *Structural and Multidisciplinary Optimization*, 45(2):153–169, 2012.

T. Dbouk. A review about the engineering design of optimal heat transfer systems using topology optimization. *Applied Thermal Engineering*, 112:841 – 854, 2017.

A.D. Ferreira and A. A. Novotny. A new non-iterative reconstruction method for the electrical impedance tomography problem. *Inverse Problems*, 33(3):035005, 2017.

A. Gersborg-Hansen, M.P. Bendsøe, and O. Sigmund. Topology optimization of heat conduction problems using the finite volume method. *Structural and Multidisciplinary Optimization*, 31(4):251–259, 2006.

S. M. Giusti, A. A. Novotny, and J. Sokołowski. Topological derivative for steady-state orthotropic heat diffusion problem. *Structural and Multidisciplinary Optimization*, 40 (1):53–64, 2010.

S.M. Giusti, Z. Mróz, J. Sokolowski, and A.A. Novotny. Topology design of thermomechanical actuators. *Structural and Multidisciplinary Optimization*, 55:1575–1587, 2017.

R. T. Haftka and Z. Gürdal. *Elements of structural optimization*. Kluwer, Dordrecht, third edition, 1992.

E.J. Haug and B. Rousselet. Design sensitivity analysis in structural mechanics.ii. eigenvalue variations. *Journal of Structural Mechanics*, 8(2):161–186, 1980.

M. Hintermüller and A. Laurain. Multiphase image segmentation and modulation recovery based on shape and topological sensitivity. *Journal of Mathematical Imaging and Vision*, 35(1):1–22, 2009.

X. Huang, Z.H. Zuo, and Y.M. Xie. Evolutionary topological optimization of vibrating continuum structures for natural frequencies. *Computers & Structures*, 88(5):357 – 364, 2010.

T. J. Ikonen, G. Marck, A. Sóbester, and A. J. Keane. Topology optimization of conductive heat transfer problems using parametric l-systems. *Structural and Multidisciplinary Optimization*, 58(5):1899 – 1916, 2018.

R. Li, Y. Tian, P. Wang, Y. Shi, and B. Wang. New analytic free vibration solutions of rectangular thin plates resting on multiple point supports. *International Journal of Mechanical Sciences*, 110:53 – 61, 2016.

J.D. Lohan, M.E. Dede, and J.T. Allison. Topology optimization for heat conduction using generative design algorithms. *Structural and Multidisciplinary Optimization*, 55 (3):1063–1077, 2017.

C. G. Lopes, R. B. Santos, A. A. Novotny, and J. Sokołowski. Asymptotic analysis of variational inequalities with applications to optimum design in elasticity. *Asymptotic Analysis*, 102:227–242, 2017.

E.F. Masur and Z. Mróz. Non-stationary optimality conditions in structural design. *International Journal of Solids and Structures*, 15(6):503 – 512, 1979.

S. A. Nazarov and J. Sokołowski. Spectral problems in the shape optimisation. Singular boundary perturbations. *Asymptotic Analysis*, 56(3-4):159–204, 2008.

S.A. Nazarov and J. Sokolowski. Shape sensitivity analysis of eigenvalues revisited. *Control and Cybernetics*, 37(4):999–1012, 2008.

J. A. Norato, M. P. Bendsøe, R. B. Haber, and D. Tortorelli. A topological derivative method for topology optimization. *Structural and Multidisciplinary Optimization*, 33 (4–5):375–386, 2007.

A. A. Novotny and J. Sokołowski. *Topological derivatives in shape optimization*. Interaction of Mechanics and Mathematics. Springer-Verlag, Berlin, Heidelberg, 2013.

A. A. Novotny, J. Sokołowski, and A. Żochowski. Topological derivatives of shape functionals. Part I: Theory in singularly perturbed geometrical domains. *Journal of Optimization Theory and Applications*, 180(2):341–373, 2019a.

A. A. Novotny, J. Sokołowski, and A. Żochowski. Topological derivatives of shape functionals. Part II: First order method and applications. *Journal of Optimization Theory and Applications*, 180(3):683–710, 2019b.

A. A. Novotny, J. Sokołowski, and A. Żochowski. Topological derivatives of shape functionals. Part III: Second order method and applications. *Journal of Optimization Theory and Applications*, 181(1):1–22, 2019c.

M. Otomori, T. Yamada, K. Izui, and S. Nishiwaki. Matlab code for a level set-based topology optimization method using a reaction diffusion equation. *Structural and Multidisciplinary Optimization*, 51(5):1159–1172, 2015.

Alexander P Seyranian, Erik Lund, and Niels Olhoff. Multiple eigenvalues in structural optimization problems. *Structural optimization*, 8(4):207–227, 1994.

A. J. Torii and J. Rocha de Faria. Structural optimization considering smallest magnitude eigenvalues: a smooth approximation. *Journal of the Brazilian Society of Mechanical Sciences and Engineering*, 39(5):1745–1754, 2017.

M. Xavier, E. A. Fancello, J. M. C. Farias, N. Van Goethem, and A. A. Novotny. Topological derivative-based fracture modelling in brittle materials: A phenomenological approach. *Engineering Fracture Mechanics*, 179:13–27, 2017.

Z. Zhang, W. Chen, and X. Cheng. Sensitivity analysis and optimization of eigenmode localization in continuum systems. *Structural and Multidisciplinary Optimization*, 52: 305–317, 2015.

(D. Ruscheinsky, F. S. Carvalho, C. T. M. Anflor) Group of Experimental and Computational Mechanics, University of Brasilia, Gama, Brazil
Email address: {dirlei,fscarvalho}@uft.edu.br, anflor@unb.br

(A.A. Novotny) Laboratório Nacional de Computação Científica LNCC/MCT, Coordenação de Métodos Matemáticos e Computacionais, Av. Getúlio Vargas 333, 25651-075 Petrópolis - RJ, Brasil
Email address: novotny@lncc.br